20th IMEKO TC4 International Symposium and
18th International Workshop on ADC Modelling and Testing
Research on Electric and Electronic Measurement for the Economic Upturn
Benevento, Italy, September 15-17, 2014

Scattering of microwaves in thin metallic films near the metal - non-metal transition

Jan Obrzut

Material Measurement Laboratory, National Institute of Standards and Technology, Gaithersburg, MD 20899, USA (jan.obrzut@nist.gov)

Abstract **– We present measurements demonstrating significant scattering of microwaves in thin metal films near the metal – non-metal percolation transition. Gold films 3 nm to 12 nm thick were characterized using patterned coplanar waveguides over a frequency range of 100 MHz to 20 GHz. Within the percolation coverage of gold nanoparticles when conductivity > 5 x 10^3 S/cm and the film properties transition from the dielectric to metallic, the microwave transmittance falls far more rapidly than the classical skin depth model would suggest. We observe a frequency-independent absorption peak of about 50 % in that range, which we believe results from an inhomogeneous localization of electromagnetic field, with no characteristic length scale. Our results demonstrate new techniques to study mechanisms of electromagnetic response of randomly structured metallic networks, and suggests the possibility of using surface-enhanced thin films for microwave applications.**

I. INTRODUCTION

Semi-continuous thin metallic films exhibit optical and electronic properties that are very different from those of continuous films or bulk materials [1, 2]. The characteristic morphology of such films develops during deposition - metallic nanoparticles nucleate to form conducting clusters mixed with dielectric voids. The size of the conducting clusters increases with increasing film thickness until a percolation threshold is passed and the film becomes conducting. In the vicinity of the percolation transition, the size of the inhomogeneities is comparable with the mean free path of the electrons and results in partial carrier localization [3]. Such films may also exhibit unexpected electromagnetic characteristics, as the carrier response may be dominated by resistive localized activated transport between grains [4].

In this report, we measure conductance and absorptance over the dielectric to metallic percolation transition using a new technique based on coplanar waveguides (CPW) [5]. This approach enables effective impedance matching and allows for measurement of the film propagation characteristics which may be accurately normalized against the CPW propagation length rather than the film thickness. The results are presented for gold nanoparticles deposited on a flat surface, which we choose as a model of 2D semi-continuous metallic film.

.

II. METHODS

A. Film preparation

Semicontinuous films were deposited by thermal evaporation directly onto CPW through a shadow mask, leaving the corresponding reference CPWs uncoated. At the same time we coated glass substrates for an optical evaluation of the films. Evaporation was performed at a vacuum pressure of 10^{-4} Pa and at a deposition rate of 0.3 Å/s. The film mass thickness was monitored during deposition by a quartz crystal oscillator.

B. Fabrication of coplanar waveguide testing structure

Coplanar waveguides with a nominal characteristic impedance value (Z_0) of 50 Ω and a propagation length (l) ranging from 450 μm to 1800 μm, were made with 10 nm Ti and 200 nm Au evaporated on 500 μm thick, 25 mm by 25 mm electronic grade alumina wafers (Fig 1). CPWs were patterned by lift off lithography. The width (w) of the central signal strip of these CPWs was 50 μm ± 0.2 μm, while the signal to ground plane spacing (s) was nominally 22 μm.

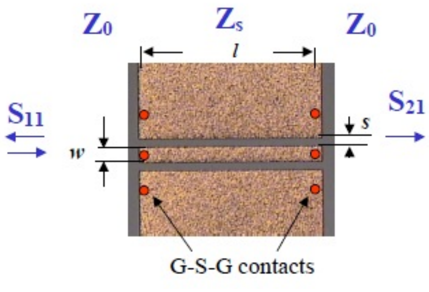

Fig.1 CPW testing structure

C. Microwave measurement and analysis

Measurements of the microwave wave scattering parameters, $\boldsymbol{S}_{11}$ and $\boldsymbol{S}_{21}$, were performed using an Agilent 8720D network analyzer in the frequency range of 1GHz to 20 GHz. The analyzer was connected to the CPW test structure with phase preserving cables from Agilent

ISBN-14: 978-92-990073-2-7

(85131-60013) and 50 Ω ground-signal-ground (GSG) air-coplanar probes (ACP-40, 100 µm pitch) from Cascade. The measurement system was calibrated using a 101-190C impedance calibration standard and WinCal calibration software from Cascade.

Parameters in bold face denote complex quantities having both magnitude and phase. After film deposition the CPW impedance changes from Z_0 to $\boldsymbol{Z}_s$. We consider the CPW test structure as a microwave network consisting of impedance discontinuity $Z_0;\boldsymbol{Z}_s;Z_0$, that is, $\boldsymbol{Z}_s$ inserted between two reference transmission lines having a real characteristic impedance Z_0 (Figure 1) where multiple wave reflection takes place at each $Z_0;\boldsymbol{Z}_s$ interface, affecting the reflection coefficient, $\boldsymbol{\Gamma}$, and transmission coefficient, $\boldsymbol{T}$ [6]. The material's properties in the specimen section of propagation length l are represented by the complex impedance $\boldsymbol{Z}_s$, and complex propagation constant $\boldsymbol{\gamma}$. The relation between the measured scattering parameters $\boldsymbol{S}_{11}$, $\boldsymbol{S}_{21}$, and $\boldsymbol{\Gamma}$, $\boldsymbol{Z}_s$ and $\boldsymbol{T}$ are given by equations (1), (2) and (3):

$$\boldsymbol{\Gamma} = b - \sqrt{b^2 - 1},\ b = \frac{S_{11}^2 - S_{21}^2 + 1}{2S_{11}} \quad (1)$$

$$\boldsymbol{Z}_S = Z_0 \frac{1+\boldsymbol{\Gamma}}{1-\boldsymbol{\Gamma}} \quad (2)$$

$$\boldsymbol{T} = \frac{\boldsymbol{S}_{11} + \boldsymbol{S}_{21} - \boldsymbol{\Gamma}}{1-(\boldsymbol{S}_{11}+\boldsymbol{S}_{21})\boldsymbol{\Gamma}} \quad (3)$$

In equation (1) $|\boldsymbol{\Gamma}| <= 1.0$. The complex transmission coefficient $\boldsymbol{T} = e^{-\gamma l}$ is related to the complex propagation constant $\boldsymbol{\gamma}$ by (4):

$$\boldsymbol{\gamma} = \ln(\boldsymbol{T}^{-1})/l \quad (4)$$

which has multiple soultions. Since $\boldsymbol{T} = |\boldsymbol{T}|e^{j\varphi}$, equation (4) can be rearranged into (5) where the real part of $\boldsymbol{\gamma}$ has an unique value, and only the imaginary part, the phase constant, has multiple values:

$$\boldsymbol{\Gamma} = \frac{\ln(|\boldsymbol{T}^{-1}|)}{l} + j\frac{2\pi\,\mathrm{n} - \varphi}{l} \quad (5)$$

The ambiguity in the phase constant can be easily eliminated by measurements on two samples with different propagation length. Having determined $\boldsymbol{Z}_s$ and $\boldsymbol{\gamma}$ the conductance, G_s can be obtained from the conventional transmission line relations (6):

$$G_s = \mathrm{Re}(\frac{\boldsymbol{\gamma}}{\boldsymbol{Z}_s}) \quad (6)$$

and, the absorption, A_s, is given by (7):

$$A_s = 1 - T_s - R_s \quad (7)$$

where the transmittance $T_s = \boldsymbol{T}\,\boldsymbol{T}^*$, reflectance $R_s = \boldsymbol{\Gamma}\,\boldsymbol{\Gamma}^*$, and $\boldsymbol{T}^*$ and $\boldsymbol{\Gamma}^*$ are the complex conjugate of the transmission and reflection coefficient respectively.

The distributed conductance G_s (Eq. 6) can be correlated with the film surface conductance (σ_s), $\sigma_s = G_s \cdot s/2$ (in units of siemens per square), where (s) is the CPW signal to ground plane spacing, here s = 22 x 10^{-4} cm (Fig 1). By normalizing σ_s to the film thickness (d), G_s can be scaled further to obtain the material's volume conductivity, $\sigma_v = \sigma_s / d$.

The combined uncertainty of scattering parameters magnitude is 0.1 dB and phase angle is 2°. The combined relative uncertainty of σ_v and A_s is within 5 %.

III. RESULTS AND DISCUSSION

Figures 2 shows the magnitude and phase of the complex scattering parameters measured for uncoated CPWs and CPWs coated with gold films with thickness increasing from 4 nm to 10 nm. The magnitude of the reflected wave, $|\boldsymbol{S}_{11}|$, for uncoated CPWs is rather small, in the range of –45 dB, indicating negligibly small insertion loss. The corresponding phase angle (plot 1 of $\boldsymbol{S}_{11}$ phase) indicates that the impedance mismatch is not significant. Uncoated CPWs show highly transmitting characteristics with $|\boldsymbol{S}_{21}|$ slightly decreasing with frequency from its maximum value of.0 dB, again indicatting that the CPWs test structures are well impedance matched.

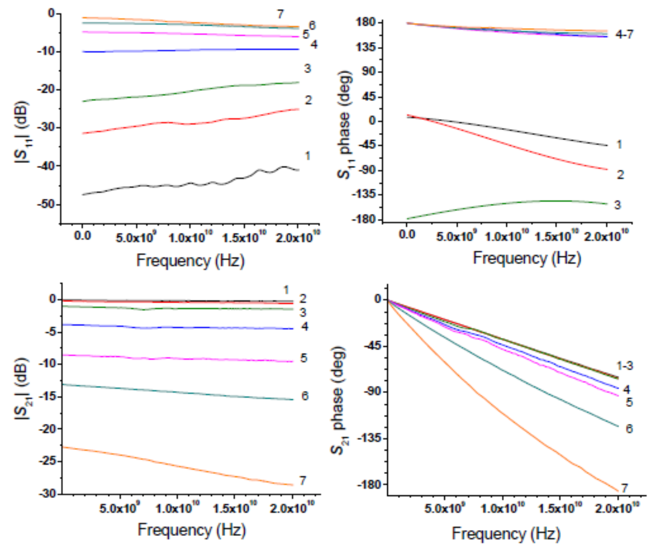

Figure 2. Magnitude and phase of scattering parameters $\boldsymbol{S}_{11}$ and $\boldsymbol{S}_{21}$ for the uncoated CPWs (1), and the following Au film thickness: (2) 4 nm, (3) 6 nm, (4) 7 nm, (5) 8 nm, (6) 9 nm, and (7) 10 nm.

There is a general tendency of conducting Au films to affect the magnitude and phase of both the $\boldsymbol{S}_{11}$ and $\boldsymbol{S}_{21}$ parameters. With increasing film thickness the magnitude of $\boldsymbol{S}_{11}$ increases, while the magnitude of $\boldsymbol{S}_{21}$ correspondingly decreases. For example, in comparison to uncoated CPWs, for a 6 nm thick Au film the $|\boldsymbol{S}_{11}|$

Certain commercial equipment, instruments, or materials are identified in this paper in order to specify the experimental procedure adequately.
Such identification is not intended to imply recommendation or endorsement by the National Institute of Standards and Technology, nor is it intended to imply that the materials or equipment identified are necessarily the best available for the purpose

value increases by several orders of magnitude, from –45 dB to about –20 dB, while $|S_{21}|$ decreases from about 0 dB to about –1.4 dB (plots 3 in Fig 2). These changes reflect the increasingly conducting character of the Au films. As the film thickness grows, $|S_{11}|$ increases towards the maximum value of 0 dB, while the phase angle approaches the value of π. An abrupt change in S_{11} phase, from –135° to + 175° when the film thickness increases from 6 nm to 8 nm, indicates a conductivity percolation transition from a dielectric to a conducting metallic state. Films thicker than 6 nm are clearly conducting, each showing $|S_{11}|$ values approaching 0 dB and similar phase angles of about π. This is characteristic of reflection from a highly conducting interface. Changes in S_{21} magnitude and phase show higher sensitivity to these thicker, more conducting films, and our measurement of both S_{11} and S_{21} accurately captures this transition from the insulating to the conducting state. It is noteworthy that the conductivity of these semicontinuous films, which are much thinner than the skin depth, is frequency independent.

Figure 3 shows the microwave reflectance R_s, transmittance T_s, and absorption A_s (Eq. 7) at 10 GHz plotted as a function of volume conductivity, which increases with increasing film thickness. Reflectance of films with conductvity $\sigma_v < 10^3$ S/cm is near zero. In this dielectric regime, the transmittance gradually decreases from 100 % to about 40 %, which is balanced by a gradual increase in absorption, A_s. Within the percolation threshold, $\sigma_v \approx 5 \times 10^3$ S/cm, the transmittance falls rapidly to zero and A_s shows a peak reaching a maximum of about 0.5, while R_s increases steeply.

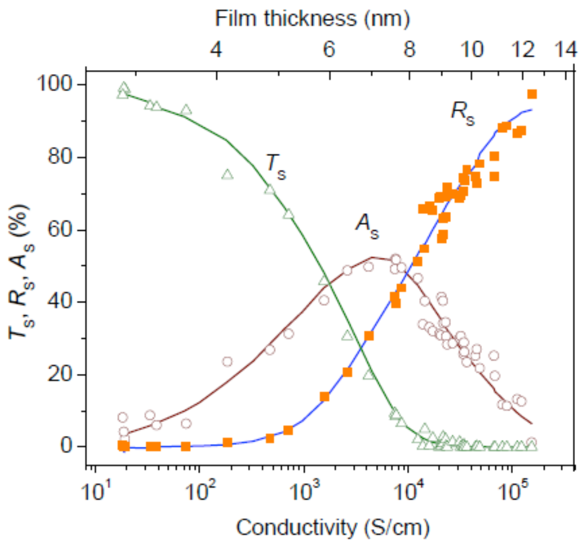

Figure 3. Microwave transmission T_s (triangles), reflection R_s (solid squares) and absorption A_s (circles) of Au films at 10 GHz in relation to conductivity ond thickness.

Above the percolation transition when $\sigma_v > 5 \times 10^3$ S/cm, A_s decays reaching a value of about 10% at $\sigma_v \approx 10^5$ S/cm, while R_s approaches a value of 90 %.

The large value of reflectance above $\sigma_v > 10^4$ S/cm (d > 10 nm) is consistent with the film forming an electrically conducting mesh. The size of the heterogeneity ξ_p in these films estimated using scaling relations from the percolation theory is about 400 nm [7]. Thus, the metallic mesh at wavelengths λ longer than ξ_p is almost totally reflecting. In Figure 3, R_s > 90 % when $\sigma_v > 10^5$ S/cm (d > 12 nm) and the network of Au nanoparticles acquire electrical characteristice of a continuous metallic film.

The frequency independent absorption peak that appears within the percolation transition (Fgure 3) is probably the most intriguing feature of these semicontinuous randomly-distributed conductive nanoparticles, which causes the transmittance to fall far more rapidly than the classical skin depth model would suggest. Table 2 illustrates this situation where attenuation $1\text{-}T_e = 1\text{-} \exp(-2d/\delta_e)$, due to skin penetration depth, $\delta_e = (\pi f \mu_r \mu_0 \sigma_v)^{-1/2}$, is several orders of magnitude smaller than the actually measured absorption A_s.

Table 1. Conductivity (σ_v), skin depth (δ_e), attenuation ($1\text{-}T_e$), measured absorbtance (A_s,)and the corresponding pentration depth δ_{As} at 10 GHz for Au films having thickness (d).

d (nm)	σ_v (S/cm)	δ_e (μm)	$1\text{-}T_e$	A_s	δ_{As} (nm)
6	33	87	1.2×10^{-4}	7×10^{-2}	200
8	2.7×10^3	9.6	1.5×10^{-3}	0.5	25
10	4.9×10^4	2.3	7.8×10^{-3}	0.21	90

For 8 nm thick films the classical attenuation model predicts absorption of 1.5×10^{-3}, since at 10 GHz $\sigma_v \approx 2.7 \times 10^3$ S/cm and the skin depth δ_e is about 9.6 μm. In comparison, the measured absorption approaches a value of 0.5 and the corresponding penetration depth $\delta_{As} = 2d/ln(1\text{-}A_s)$ decreases to about 25 nm.

The experimental microwave scattering data suggest that the interaction of microwaves with randomly distributed conductive particles leads to localized resonant modes within the film, where the resonant wave is confined in a dimension comparable with the particle grain size, which is in the range of 20 nm to 100 nm.

In an attempt to explore the origin of the microwave absorption in more detail we examine the phase characteristic of the reflected wave, S_{11} shown in Figure 2. The phase angle (φ) of the scattering parameter S_{11} is negative, consistent with the predominantly dielectric character of the films thinner than 6 nm below the percolation threshold. With film thickness increasing beyond the percolation threshold and with increasing conductivity, the phase angle changes from negative to positive values by about π. This indicates a transition from a capacitive (X_C) to inductive reactance (X_L) evidencing a quarter-wavelength resonance, which leads to resonant power dissipation. The film response may be formally described as equivalent to a distribution of RL circuits or electrically shorted transmission lines, having length of λ_g /4. The wide range of conductivity values over which the anomalous absorption is observed (Figure 3) indicates a broad distribution of the effective guided wavelengths. The guided wavelength is typically shorter than the incident free space wavelength λ_0 by a factor of the effective relative dielectric constant $(\varepsilon_r)^{0.5}$. In randomly distributed metallic and dielectric clusters, ε_r diverges near the dielectric to conductor percolation threshold [8] and may locally increase over several orders of magnitude [4, 9], compressing λ_g to a length scale comparable with the grain size. The ratio of the internal film resistance and impedance, $|R/Z|$ normalizes the resonant absorption such that when $Z = R$, $A_s = 1.0$ [10]. When A_s attains a peak value ≈ 0.5, the film reactance is inductive ($Z = R + X_L$) and $R/(R + X_L) \approx 0.5$. Thus a significant portion of the injected microwave power is stored in the magnetic field until dissipated.

This anomalous absorption is frequency independent and therefore in contrast to plasmonic resonance, the inhomogeneous localization of electromagnetic field at microwave frequencies apparently has no characteristic length scale. Rather, the universal percolation exponents of the conducting particles network govern it. By tuning the particle concentration towards the percolation threshold the structure of the semicontinuous film transitions from an electric to magnetic energy concentrator. These results quantify absorption of semicontinuous films near metal – non-metal transition and clarify their considerably higher value compared to continuous metallic films.

IV. SUMMARY

We present a new technique to effectively allow coupling of microwaves to nanostructured films over a broad frequency range. Our results provide strong evidence of large resonant absorption within the percolation transition. The resonant wave is confined in a dimension comparable with the particle grain size rather than the film thickness. The effective attenuation distance of microwaves is about 25 nm to 200 nm, several orders of magnitude shorter than the classical skin depth model predicts. The films attain a maximum absorption of about 0.5 slightly above the percolation threshold, when the film thickness is about 8 nm and conductivity about 5 x 10^3 S/cm. By increasing the particle concentration the film reactance becomes inductive and the structure transitions from an electric to magnetic energy concentrator. The effect opens the possibility of manipulating microwave energy in sub-wavelength structures through engineering neworks of metallic nanoparticles.

REFERENCES

[1] D. Berthier, J. Peiro, “Anomalous Infrared Absorption of Nanocermets in the Percolation Range”, J. Phys. Condens. Matter vol. 10, 1998, pp. 3679-3694.

[2] M. Walther, D. G. Cooke, C. Sherstan, M. Hajar, M. R. Freeman, F. A. Hegmann, “Terahertz Conductivity of Thin Gold Films at the Metal-Insulator Percolation Transition” Phys. Rev. B vol. 76, 2007, pp.125408-1-125408-9.

[3] V. Krachmalnicoff, E. Castanie, Y. De. Widde, R. Carminati, “Fluctuations of the Local Density of States Probe Localized Surface Plasmons in Disordered Metal Films” Phys. Rev. Lett. Vol.105, 2010, pp/ 183901-1-183901-4.

[4] V. A. Shubin, A. K. Sarychev, J. P. Clerc, V. M. Shalev, “Local Electric and Magnetic Fields in Semicontinuous Metal Films: Beyond the Quasistatic Approximation” Phys. Rev. B, vol. 62, 2010, pp. 11230-11244.

[5] J. Obrzut, O. Kirillov, “Microwave Conductance of Semicontinuous Metallic Films from Coplanar Waveguide Scattering Parameters” 2013 IEEE International Instrumentation and Mesurement Technology Conference Proceedings, Minneapolis, MN, May 6-9, 2013, pp 912-916.

[6] J. Obrzut, “General Analysis of Microwave Network Scattering Parameters for Characterization of Thin Film Materials” Measurement J., vol. 46, 2013, pp. 2963-2970.

[7] J. Obrzut, J. F. Douglas, O. Kirilov, F. Sharifi, J. A. Liddle,” Resonant Microwave Absorption in Thermally Deposited Au Nanoparticle Films Near Percolation Coverage”, Langmuir, vol. 29, 2013, pp. 9010-9015.

[8] A. L. Efros, B. I. Sklovsii, “Critical Behavior of Conductivity and Dielectric Constant near the Metal-Non-Metal Transition Threshold. *Phys. Stat. Sol. B* vol 76, **1976,** pp. 475 – 485.

[9] R. F. Wu, W. Pan, S. L. Shi, R. B. Han, “Critical Behaviors of the Conductivity and Dielectric Constant of Ti3SiC2/Al2O3 Hybrids” *J. Appl. Phys.* Vol. 102, 2007, p. 056104.

[10] M Sucher, “Measurement of Q”, In Handbook of Microwave Measurements, Microwave Measurements; Sucher, M.; and Fox, J., Eds.; Polytechnic Press of the Polytechnic Institute of Brooklyn: New York, 1963; p. 420.